Office de la Propriété Intellectuelle du Canada
Un organisme d'Industrie Canada

Canadian Intellectual Property Office
An agency of Industry Canada

CA 2302121 A1 2001/09/27

(21) 2 302 121

(12) DEMANDE DE BREVET CANADIEN
CANADIAN PATENT APPLICATION

(13) A1

(22) Date de dépôt/Filing Date: 2000/03/27

(41) Mise à la disp. pub./Open to Public Insp.: 2001/09/27

(51) Cl.Int.^{7}/Int.Cl.^{7} G01R 1/067, G01N 15/02, G01N 27/00

(71) Demandeur/Applicant:
LIMCA RESEARCH INC., CA

(72) Inventeurs/Inventors:
Guthrie, Roderick I.L., CA;
LI, MEI, US

(74) Agent: ROGERS, STANLEY J.

(54) Titre : SONDES DE MESURE DE LA QUALITE D'UN METAL FONDU
(54) Title: LIQUID METAL QUALITY SENSORS

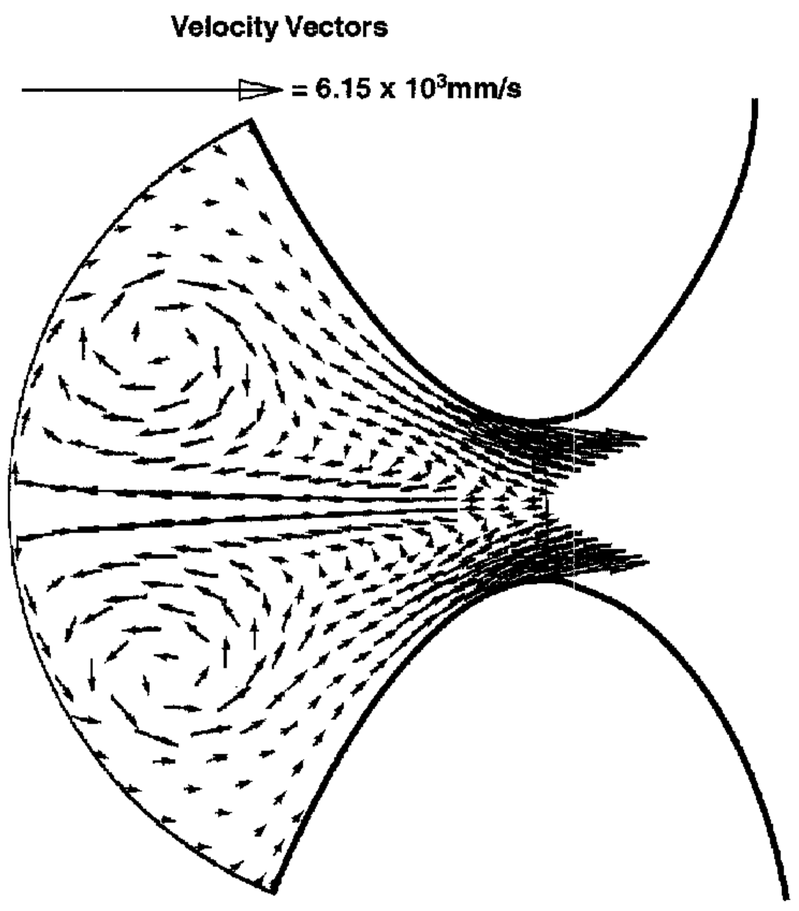

(57) Abrégé/Abstract:
The present invention relates to quality control of liquid metals and an apparatus for monitoring, on line, the flowing molten metal. It has long been a desirable goal to be able to measure the quality of liquid metals in terms of the numbers and sizes of inclusions within a melt. Since the 1960s, owing to the increasing use of foil and thin gauge products such as the aluminium beverage cans, aluminium companies such as Reynolds and Alcan had attempted to develop ultrasonic methods to detect inclusions in molten aluminium. These met with little success, Alcan's twenty years of effort being abandoned following the successful introduction of the LiMCA, trade-mark of Limca Research Inc., (Liquid Metal Cleanliness Analyser) method by Doutre and Guthrie. This technique relies on the Electric Sensing Zone Principle (ESZ), and was well known for aqueous systems, since the Coulter patents of 1954. The equivalent LiMCA method for liquid metals is also based on the ESZ principle, and is now in world-wide use in cast houses making critical quality alloys (AA3001, 3004) for the production of aluminium beverage cans, sheet and lithographic plates. The commercial equipment is manufactured under licence, by Bomem, Quebec City, and is able to monitor, on line, the quality (number and size distribution of inclusions) of molten aluminium flowing from the holding furnaces through a launder, into the moulds of a DC (Direct Chill) casting machine. See U. S. Patent 4,555,662, Doutre and Guthrie, issued November 26, 1985, and U. S. Patent 4,600,880, for instance. Several other patents have since been obtained by Alcan International.

"LIQUID METAL QUALITY SENSORS"

The present invention relates to quality control of liquid metals and an apparatus for monitoring, on line, the flowing molten metal.

It has long been a desirable goal to be able to measure the quality of liquid metals in terms of the numbers and sizes of inclusions within a melt. Since the 1960s, owing to the increasing use of foil and thin gauge products such as the aluminium beverage cans, aluminium companies such as Reynolds and Alcan had attempted to develop ultrasonic methods to detect inclusions in molten aluminium. These met with little success, Alcan's twenty years of effort being abandoned following the successful introduction of the LiMCA, trade-mark of Limca Research Inc., (Liquid Metal Cleanliness Analyser) method by Doutre and Guthrie. This technique relies on the Electric Sensing Zone Principle (ESZ), and was well known for aqueous systems, since the Coulter patents of 1954. The equivalent LiMCA method for liquid metals is also based on the ESZ principle, and is now in world-wide use in cast houses making critical quality alloys (AA3001, 3004) for the production of aluminium beverage cans, sheet and lithographic plates. The commercial equipment is manufactured under licence, by Bomem, Quebec City, and is able to monitor, on line, the quality (number and size distribution of inclusions) of molten aluminium flowing from the holding furnaces through a launder, into the moulds of a DC (Direct Chill) casting machine. See U. S. Patent 4,555,662, Doutre and Guthrie, issued November 26, 1985, and U. S. Patent 4,600,880, for instance. Several other patents have since been obtained by Alcan International.

One of the major concerns within aluminum industry is metal cleanliness. This relates to the number and size distribution of nonmetallic inclusions suspended within a melt. Inclusions whose diameter exceed 15μm in aluminum alloys are considered potentially detrimental. Their presence within a solidified product can lead to various types of defects which, in turn, can increase breakage or rejection rates. For example, the production of beverage can bodies is very sensitive to the presence of any inclusions within the can walls, whose dimensions are in the order of 80μm thick. Harder, larger inclusions (~ 60μm) can cause the metal to tear during deep drawing or the can to perforate when its content is pressurized.

Prior to the development of the LiMCA system at McGill University in the early 1980's, it was not possible to measure inclusions, *in situ*, in liquid metals. Compared with other techniques, such as sedimentation, filtration and metallography, which require considerable amounts of labor and time, the LiMCA method has the advantage of providing not only information on the volume concentration of inclusions, but also on the size distribution of inclusions immediately and quantitatively.

The LiMCA technique is based on the Electric Sensing Zone (ESZ) principle, in which a constant current is maintained between two electrodes that are separated physically by an electrically insulating sampling tube. A 300μm orifice within the non-conductive tube wall allows molten aluminum to flow into, and out of, the tube in a cyclic manner. This cycling sequence is controlled pneumatically by a differential

pressure control system. When a non-conductive particle passes through the 300μm orifice, the resistance within the ESZ rises, causing a voltage pulse.

Since every particle registers a pulse when passing through the ESZ, and non-conductive particles of the same size but of different type give rise to voltage pulses of the same magnitude, it has previously been impossible to discriminate between different types of inclusions within a melt. In the aluminum industry, proprietary degassing units generate microbubbles and microdroplets of salt in molten aluminum. These microbubbles and microdroplets interfere with the LiMCA probe and its inclusion counts. In practice, microbubbles are relatively harmless compared to hard solid inclusions, and one therefore needs to distinguish one from the other in terms of a metal quality control point of view. In order to attempt particle discrimination, the analogue LiMCA system was updated with Digital Signal Processing (DSP) technology to determine whether more information could be extracted from particle signals besides pulse height. Using the McGill DSP system, each pulse was characterized by not only the peak height, but six other pulse parameters (start slope, end slope, time to maximum voltage, total signal duration, start time and end time). A previous study using an aqueous based ESZ system confirmed for the first time, both theoretically and experimentally, that inclusions of different density could be discriminated on the basis of differently shaped voltage transients generated during their passage through the electric sensing zone.

Besides monitoring the quality of liquid metals in terms of the number and size distribution of non-conductive extraneous inclusions, the LiMCA technology has also

been extended to the analysis of grain refining additions of titanium diboride (TiB_2) to aluminum silicon casting alloys. Negative voltage pulses were observed using TiB_2 grain refiners containing less than 2% Ti, since TiB_2 is more conductive electrically than molten aluminum. For monitoring these more conducting particles, a relationship between the electrical conductivity of a particle and its induced signal needs to be defined.

Furthermore, the successful operation of LiMCA system depends on a procedure termed "conditioning", which involves passing a 200–300 Amperes electric current through the orifice for about 300 ms before taking a new sample when inflow rates decrease, or when voltage baseline instabilities are observed. In practice, the application of this high current, compared to the 60 Amperes working current, usually stabilizes the baseline of the signal, presumably by removing any obstructions to molten aluminum flowing through the orifice. The mechanism for this conditioning effect is a key to LiMCA's successful implementation in melts of aluminum but still needs be clarified.

Electric Sensing Zone (ESZ) Principle

The theoretical basis of the LiMCA technique is the Electric Sensing Zone Principle (Figure 7). A conductive liquid medium is separated by an electrically insulated wall. A small opening in the wall submerged in the liquid connects the two parts of the medium. A constant DC voltage is applied across the orifice, while the liquid is forced to flow through it. In Figure 1 , a cross-section view of a cylindrical orifice with length L and diameter D is illustrated. Conductive fluid is flowing through the orifice with constant flow rate Q and electric current I. Because of the geometrical confinement of the orifice, the electric field is intensified inside the orifice and thus becomes very sensitive to the change of the electrical property of the conductive fluid flowing through the orifice. The volume inside the orifice is called the Electric Sensing Zone, ESZ for short. When a non-conductive particle passes through the orifice with the fluid flow, the overall resistance of the orifice is increased momentarily and can be detected as a voltage pulse. A non-conductive particle with diameter d suspended in the fluid is shown in Figure 7 as it

passes through the orifice. The position of the particle is labeled with time *t1*, *t2*,.... Under the following assumptions:

1. Inclusions are spherical
2. Inclusions are non-conductive
3. The orifice is cylindrical with diameter D and length $L(>> D)$
4. Only one inclusion passes through the orifice at a given time
5. The current density within the ESZ is constant

The voltage change ΔV is related to the volume of the particle by **Equation 1.1** [DeBlois and Bean 70]. This equation is used as a basic relation to predict the size of particle from the voltage change ΔV.

$$\Delta V = I\frac{4\rho d^3}{\pi D^4} f(d/D) \qquad (1.1)$$

where

$$f(d/D) = \frac{1}{1-0.8(d/D)^3}$$

The LiMCA sensor is designed to have an ESZ of a certain shape and to catch and monitor the voltage change due to a particle passing through the ESZ. The design of the probe and the materials used to construct it depend on the metal or alloy to be evaluated and analyzed.

Figure 2 shows a typical LiMCA sensor for use in molten aluminum and its alloys. It consists of an electrically-insulated tube with a small orifice at the side wall near the bottom and two electrodes, one inside, the other outside the tube facing the orifice. The tube is made of Kimax glass, and the electrodes are made of steel. A smoothly-curved orifice is desirable for a stable metal flow through the orifice. This is **essential for stable signal.** A glass blowing technique is applied to make the orifice.

It is an aim of the present invention to provide an improved LiMCA device for monitoring the quality of aluminum and other metals.

The invention relates to the interaction of the shape of the sensory zone at the orifice with the flow of electric current that causes a self-induced magnetic field whose spatial geometry can be manipulated to create a flow reversal at high currents characteristic for the conditioning effect. By having the walls forming the nip at the orifice in a parabolic shape, the pressure is caused to rise to compensate for the magnetic pinch effect, that is, the self-induced electromagnetic force which is greatest at the walls and diminishes to zero at the center of the orifice. This, however, is counter-balanced by a rise in pressure towards the central axis. Since the current density at the throat of the orifice is much greater than a point outside the orifice, the pressure at the center is greater than the static pressure so a flow reversal is caused that breaks up any accumulating bridge of inclusions upstream of the orifice and scours them out owing to the high velocities along the side walls of the zone of the orifice.

Having thus generally described the nature of the invention, reference will now be made to the accompanying drawings, showing by way of illustration, a preferred embodiment thereof, and in which:

Fig. 1 is a schematic diagram showing the LiMCA technique with a cylindrical orifice in accordance with the prior art;

Fig. 2 is a schematic diagram showing the LiMCA sensor in a molten bath according to the prior art;

Fig. 3 shows an enlarged schematic view of the orifice for the probe for the LiMCA device having parabolically curved surfaces conducive to the magnetic pinch;

Figs. 4, 5, 6a to 6d, and 7 are diagrams showing the characteristics of the present invention;

Fig. 8 is a graph plotting the flow of the inclusions; and

Fig. 9 shows a schematic view of a typical LiMCA sensor.

The present study considered the dynamic motions of particles entrained within molten aluminum flowing through the ESZ, and corresponding changes in electrical resistance within the ESZ. A two dimensional simulation using a cylindrical coordinate system was employed. As shown in Figure 4 , the position of the particle is designated as (x_p, y_p), where x and y are the respective axial and radial coordinates. L_{tube} is the thickness of the sidewall of the sampling tube, L is the length of the ESZ, R is the radius of the throat at the center of the ESZ, I is the electric current flowing within the ESZ, and U_0 is the inlet fluid flow velocity.

II.1. Electric Sensing Zone (ESZ) Principle

LiMCA is based on the electric sensing zone principle. The central theoretical problem of the principle is determining the resistance change of the ESZ by the insertion of an inclusion inside.

Maxwell showed that the resistance $R_{ESZ-particle}$ of the ESZ with an inclusion inside is given by:

$$R_{ESZ-with-particle} = \rho_{eff} \int \frac{dx}{A(x)} \qquad (1)$$

where $A(x)$ is the area of the cross-section of the ESZ and ρ_{eff} is the effective electrical resistivity of a compound conducting media. The media is composed of one continuous material of resistivity ρ_e and sparsely distributed spherical inclusions of resistivity ρ_{e_p}. When the particles are sufficiently scattered so that the distance between each other is large enough so as to not disturb the course of the surrounding current, then ρ_{eff} can be expressed as:

$$\rho_{eff} = [\frac{2\rho_{e_p} + \rho_e + f(\rho_{e_p} - \rho_e)}{2\rho_{e_p} + \rho_e - 2f(\rho_{e_p} - \rho_e)}]\rho_e \qquad (2)$$

where f is the volume fraction of inclusions contained within the ESZ.

In a cylindrical orifice used in the theoretical pulse calculation, the resistance of the ESZ without the introduction of inclusion is given by :

$$R_1 = \frac{4\rho_e L}{\pi D^2} \qquad (3)$$

where D and L are the diameter and length of the ESZ, respectively.

If an inclusion of diameter d is introduced, then the volume fraction of this inclusion to the ESZ volume is:

$$f = \frac{2d^3}{3D^2 L} \qquad (4)$$

The resistance of the ESZ with a small inclusion within it is given by:

$$R_2 = \frac{4\rho_{eff} L}{\pi D^2} \qquad (5)$$

Thus, the change in resistance

$$\Delta R = R_2 - R_1 = \frac{4L}{\pi D^2}(\rho_{eff} - \rho_e) \qquad (6)$$

is determined by the dimensions of the orifice, the size of the particle, and the electrical resistivity of both the particle and the liquid media.

II.1.1. Non-conductive particle ($\rho_{e_p} >> \rho_e$)

For a non-conductive inclusion, the expression for ρ_{eff} can be approximated as:[9)]

$$\rho_{eff} = \frac{1}{2}(\frac{2+f}{1-f})\rho_e \qquad (7)$$

Expanded into a power series, Equation (7) becomes

$$\rho_{eff} = \rho_e(1+\frac{3}{2}f+\frac{3}{2}f^2+\cdots) \qquad (8)$$

Since f is very small, present calculations only consider the first two terms and ignore the higher order ones. Substituting Equations (4) into (8) and then into Equation (6):

$$\Delta R_{non-conductive} = \frac{4\rho_e d^3}{\pi D^4} \qquad (9)$$

This expression is used in the Coulter Couter for aqueous systems and the LiMCA for liquid metal systems for non-conducting particle measurement.

II.1.2. Perfectly conducting particle ($\rho_{e_p} << \rho_e$)

For a perfectly conducting particle, the expression for ρ_{eff} can be approximated as:

$$\rho_{eff} = \frac{1}{2}(\frac{1-f}{1+2f})\rho_e \qquad (10)$$

Expanded into a power series, Equation (10) becomes

$$\rho_{eff} = \rho_e(1-3f+6f^2+\cdots) \qquad (11)$$

Ignoring higher order terms, Equations (11) is substituted into Equation (6):

$$\Delta R_{conductive} = -\frac{8\rho_e d^3}{\pi D^4} \qquad (12)$$

It can be seen that the voltage pulse generated by a perfectly conducting particle is negative, opposite to that of a non-conductive particle, and has a peak resistive height two times that of a non-conducting particle of the same size.

II.1.3. TiB_2 particle in molten aluminum

In accordance with the procedure used in deriving the resistance change of the ESZ with a non-conductive or perfectly conducting particle inside, the change in the resistance of ESZ in molten aluminum with a TiB_2 particle inside can be obtained, for the properties shown in Table I, as follows:

$$\Delta R_{TiB_2} = -\frac{32}{43}\left(\frac{4\rho_e d^3}{\pi D^4}\right) \qquad (13)$$

It is seen that the voltage pulse should be negative because TiB_2 is more conductive than molten aluminum, and that the height of the voltage peak should be about three fourths of that for a non-conductive particle of the same size.

II.2. The Flow Field in the ESZ

In order to predict the flow behavior of molten aluminum entering the converging section of a typical sensing zone, the metal was taken to be incompressible, with constant properties, and the flow was considered laminar and steady, in keeping with practical operating conditions. For LiMCA systems, the orifice (ESZ) Reynolds number is about 1700 based on orifice diameter. Given these assumptions, the problem may be stated by writing the continuity and Navier-Stokes equations. Owing to the high electrical current

densities involved with LiMCA systems, the Lorentz force $\bar{F}_e(F_{e_x}, F_{e_y})$ constituting a body force is important and needs inclusion in the latter equation:

$$\bar{\nabla} \bullet \bar{u} = 0 \tag{14}$$

$$\bar{u} \bullet \bar{\nabla}\bar{u} = -\frac{\nabla p}{\rho_f} + \nu_f \nabla^2 \bar{u} + \frac{1}{\rho_f}\bar{F}_e \tag{15}$$

where $\bar{u}(u, v)$ is the fluid velocity vector, p is the pressure, ρ_f and ν_f are the density and kinematic viscosity of the fluid, respectively. $\bar{F}_e$, the Lorentz force, is defined by the following equation:

$$\bar{F}_e = \bar{J} \times \bar{B} \tag{16}$$

where $\bar{J}(J_x, J_y)$ is the electric current density, and $\bar{B}$ is the self-induced magnetic field within the ESZ. To solve for $\bar{J}$ and $\bar{B}$, Maxwell's equations need to be solved. In the present work, $\bar{J}$ is obtained through the Laplace equation:

$$\frac{\partial^2 \varphi}{\partial x^2} + \frac{1}{y}\frac{\partial}{\partial y}(y\frac{\partial \varphi}{\partial y}) = 0 \tag{17}$$

where φ is the electrical potential. The current density can be calculated from Ohm's law which is described in equations (18) and (19):

$$J_x = -\sigma_e \frac{\partial \varphi}{\partial x} \tag{18}$$

$$J_y = -\sigma_e \frac{\partial \varphi}{\partial y} \tag{19}$$

where σ_e is the electrical conductivity. For molten aluminum, this is $4.0\times10^6\ \Omega^{-1}m^{-1}$. The self-induced magnetic field is derived from Ampere's law with μ_0 as the magnetic

permeability of free space ($\mu_0 = 4\pi \times 10^{-7}\ \ Wb/A-m$):

$$B_\theta = \frac{\mu_0}{y}\int_0^y J_z \xi d\xi \tag{20}$$

where θ is the azimuthal and ξ is the radial co-ordinate in the cylindrical coordinate system.

The ESZ of LiMCA system in molten aluminum is shown in Figure 4 , where EWOO' is the computational domain used in this study. The boundary-fitted grid employed are shown in Figure 5 . The inlet boundary was taken to be a spherical cap centered at point C, this being the intersection of the central axis and the cone tangential to the ESZ wall at the edge E. The outlet boundary for the flow of the fluid and electricity was taken to be the central cross section (the throat OO') of the orifice. The boundary conditions applied were zero-slip along and zero electric current flux across the insulating ESZ wall. At the inflow boundary, the fluid velocity and the electric current density were taken to be both uniform and normal to the spherical cap boundary. At the outflow boundary, the electrical potential was assumed constant, and the exit fluid velocity gradient zero. Iterative corrections were made in the numerical calculations to match the mass outflow rate with the inflow rate, so as to respect continuity. Beyond the throat of the ESZ, jet flow was assumed, that is, the fluid flow ignores the diverging sidewalls on the exit side of the ESZ, and simply passes on through with an axial velocity distribution of the same as that at the throat.

II.3. The Equation of Motion for Inclusions

The motion of inclusions within the flow is complicated because it is not only

equation for the motion of particles was solved employing a fourth order Runge-Kutta method. The history integral needs special attention because of the singular point at the upper integration limit. It is evaluated through the following equation:

$$\int_0^t \frac{\dot{U}}{f(t-\tau)}d\tau = \int_0^{n\Delta t} \frac{\dot{U}}{f(t-\tau)}d\tau = \frac{\Delta t}{6}\sum_{i=1}^{n-1}\left[\frac{\dot{U}_{i-1}}{f(n\Delta t-(i-1)\Delta t)} + \frac{2(\dot{U}_{i-1}+\dot{U}_i)}{f(n\Delta t-(i-0.5)\Delta t)} + \frac{\dot{U}_i}{f(n\Delta t-i\Delta t)}\right] + \frac{0.9\Delta t}{6}\left[\frac{\dot{U}_{n-1}}{f(\Delta t)} + \frac{2(\dot{U}_{n-1}+\dot{U}_n)}{f(0.55\Delta t)} + \frac{\dot{U}_n}{f(0.1\Delta t)}\right] + \frac{0.1\Delta t}{2}\left[\frac{8\sqrt{2}}{3}\frac{\dot{U}_n}{f(0.05\Delta t)} - \frac{4}{3}\frac{\dot{U}_n}{f(0.1\Delta t)}\right] \quad (26)$$

with $\dot{U} = \frac{d(\vec{u}-\vec{u}_p)}{d\tau}$, $f(t-\tau) = (t-\tau)^{1/2}$. Δt is the time step whose value is set as $10^{-5}s$ to maintain the accuracy of the calculation.

III. RESULTS AND DISCUSSION

III.1. Fluid Flow and Electromagnetic Fields

The calculation of the fluid flow and electromagnetic fields inside the ESZ for aluminum melts is based on probe dimensions, operating conditions and the physical properties of the melt listed in Table I. The distributions of electrical potential, electric current density, self-induced magnetic flux density, and specific electromagnetic force within the ESZ, are shown in Figures 6a through 6d, respectively. As can be seen from Figure 6a, the isopotential along the central cross section of the orifice has its highest value, where the current flow from the inner positive electrode enters the throat of the ESZ. The electrical potential gradient is very high near the throat of the orifice and drops gradually towards the entrance or exit of the orifice. The voltage drop over the whole orifice is approximately 0.105 volts. This potential distribution gives rise to the

electric current density shown in Figure 6b . Corresponding to the potential distribution, the current density is very high near the central region of the orifice, and decreases with increasing distance from the throat. The self-induced magnetic flux within the orifice (Figure 6c) increases from the central axis to the wall. The interaction of the electric current and its induced magnetic flux results in an electromagnetic force whose distribution is shown in Figure 6d . It can be seen that the stronger electric current density and magnetic flux density near the throat of the orifice give rise to much stronger electromagnetic forces there than in the entrance or exit regions. The electromagnetic force is high near the wall, but decreases with decreasing distance from the central axis, becoming virtually and theoretically, zero along the central axis. In this force field, particles suspended in molten aluminum that are electrically non-conductive experience a force in the opposite direction, and are squeezed out of the molten metal, while particles that are electrically more conductive than molten aluminum experience a force in the same direction, and are pushed towards the central axis.

Further computations as shown in Fig. 7 have revealed that the conditioning current of 250 to 300 amperes, needed for achieving stable metal quality readings with a 300 μm orifice, which is made prior to each measurement, can generate a complex flow reversal. The phenomenon is a result of the magnetic pinch effect interacting with a precise shape of the entrance to the ESZ. The combination creates a pressure buildup in the orifice, causing a strong flow reversal that scours away any debris or residual buildups of inclusions at the entrance of ESZ.

Fig. 8 shows computed trajectories of insulating and perfectly conducting inclusions entering the parabolically shaped ESZ at a radial distance of 1.7 R, where R is the radius of the vena contracta (150 microns). Since the major fraction of inclusions are generally non-conducting, they experience strong radial forces at 60 amps applied current, causing them to veer towards the side walls of the sensing zone. They may then collide, attached or rolled, producing spurious electrical signals. By limiting the length of the particle deflection zone through the use of a parabolically shaped entrance region, the passed-through fraction of inclusions can be significantly enhanced.

The embodiments of the invention in which an exclusive property or privilege is claimed are defined as follows:

1. An insulating wall of a vessel for forming part of a fluid or molten fluid monitoring device which comprises two electrodes with a constant current, the insulating wall defining a 300 μm orifice defined by the vessel wall and the vessel wall, forming the orifice, having a parabolic cross-section.

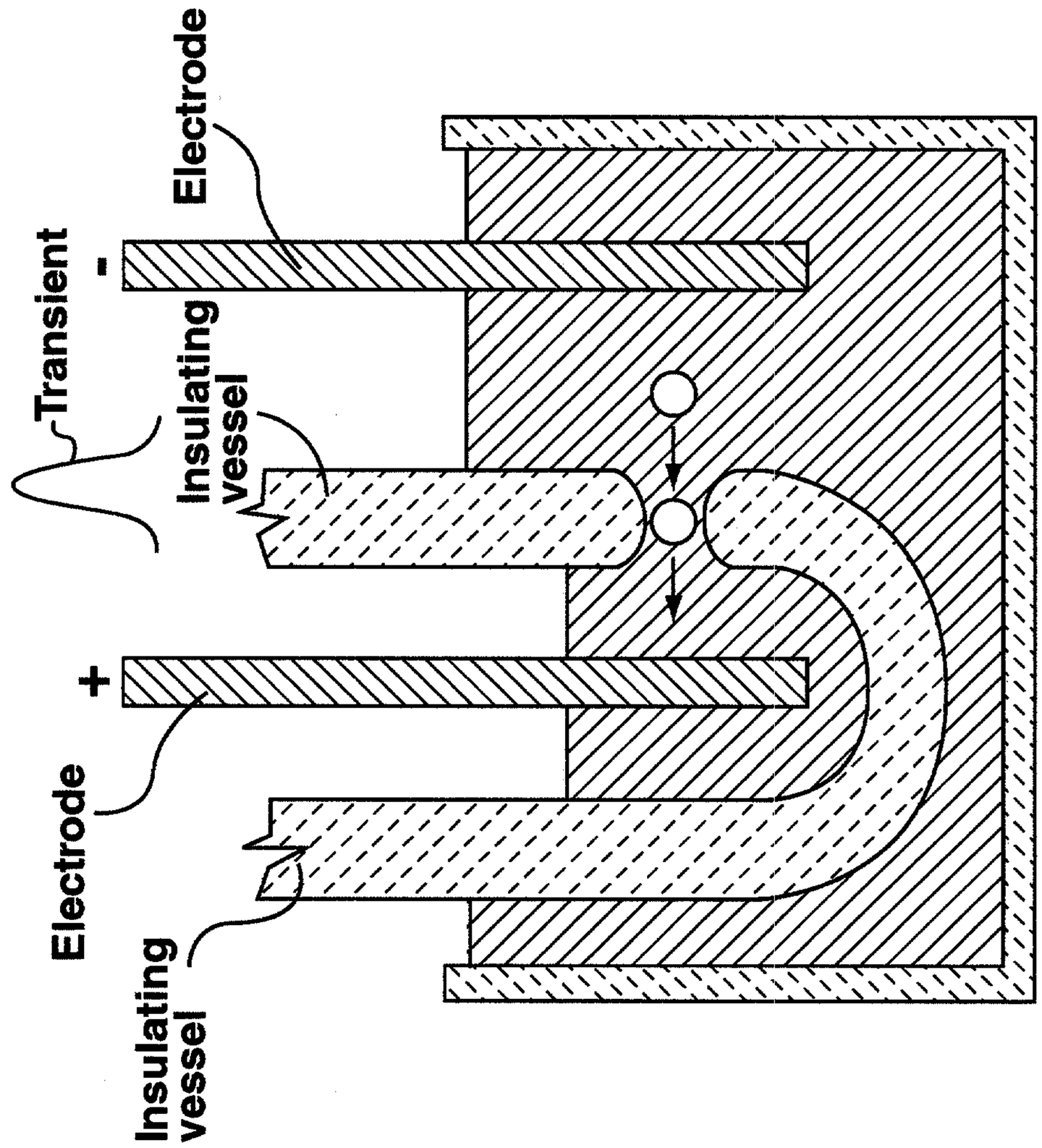

FIG. 2 (prior art)

FIG. 1 (prior art)

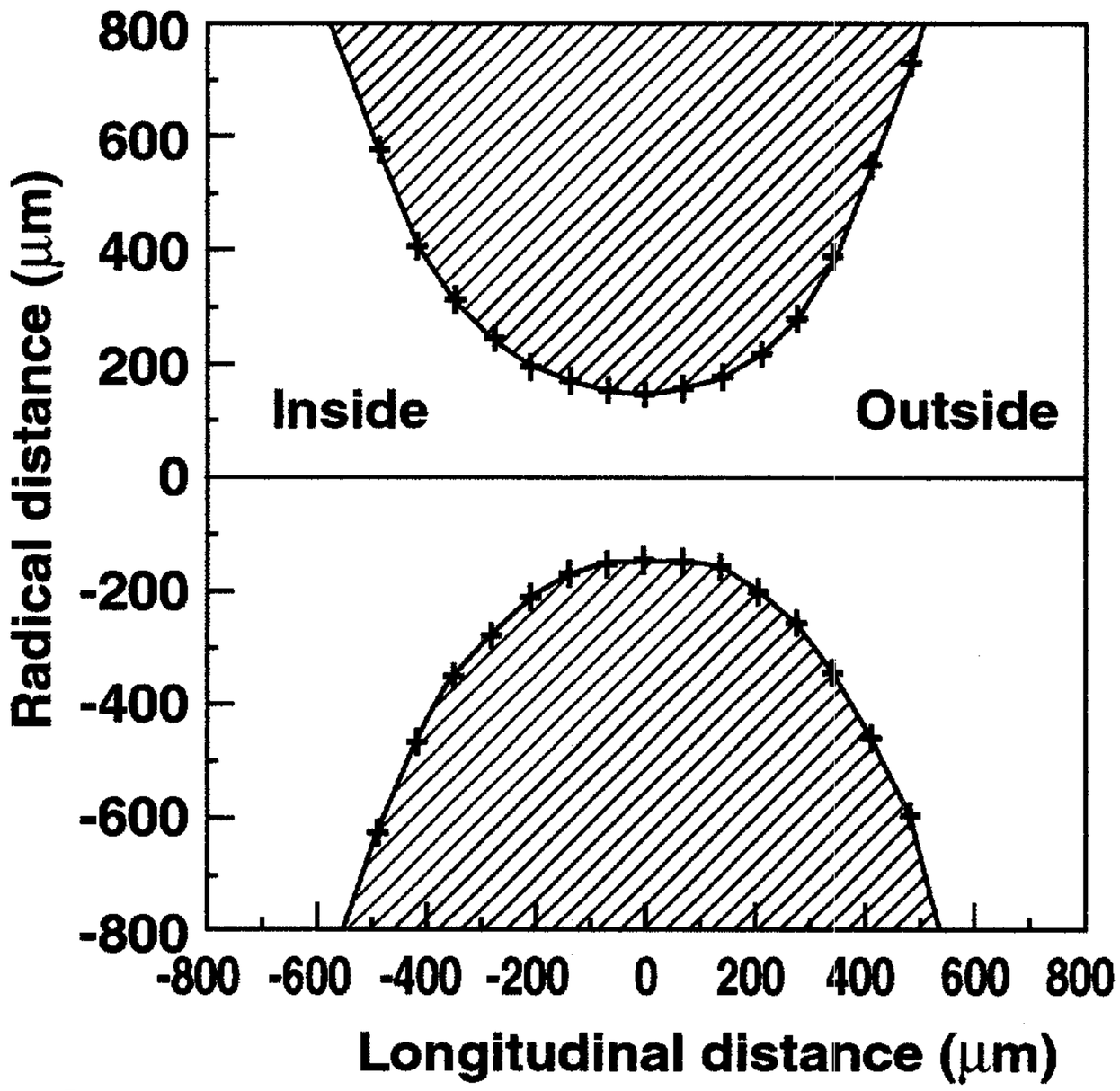
800
600
400
200
0
-200
-400
-600
-800
Radical distance (μm)
Inside
Outside
-800 -600 -400 -200 0 200 400 600 800
Longitudinal distance (μm)

FIG. 3

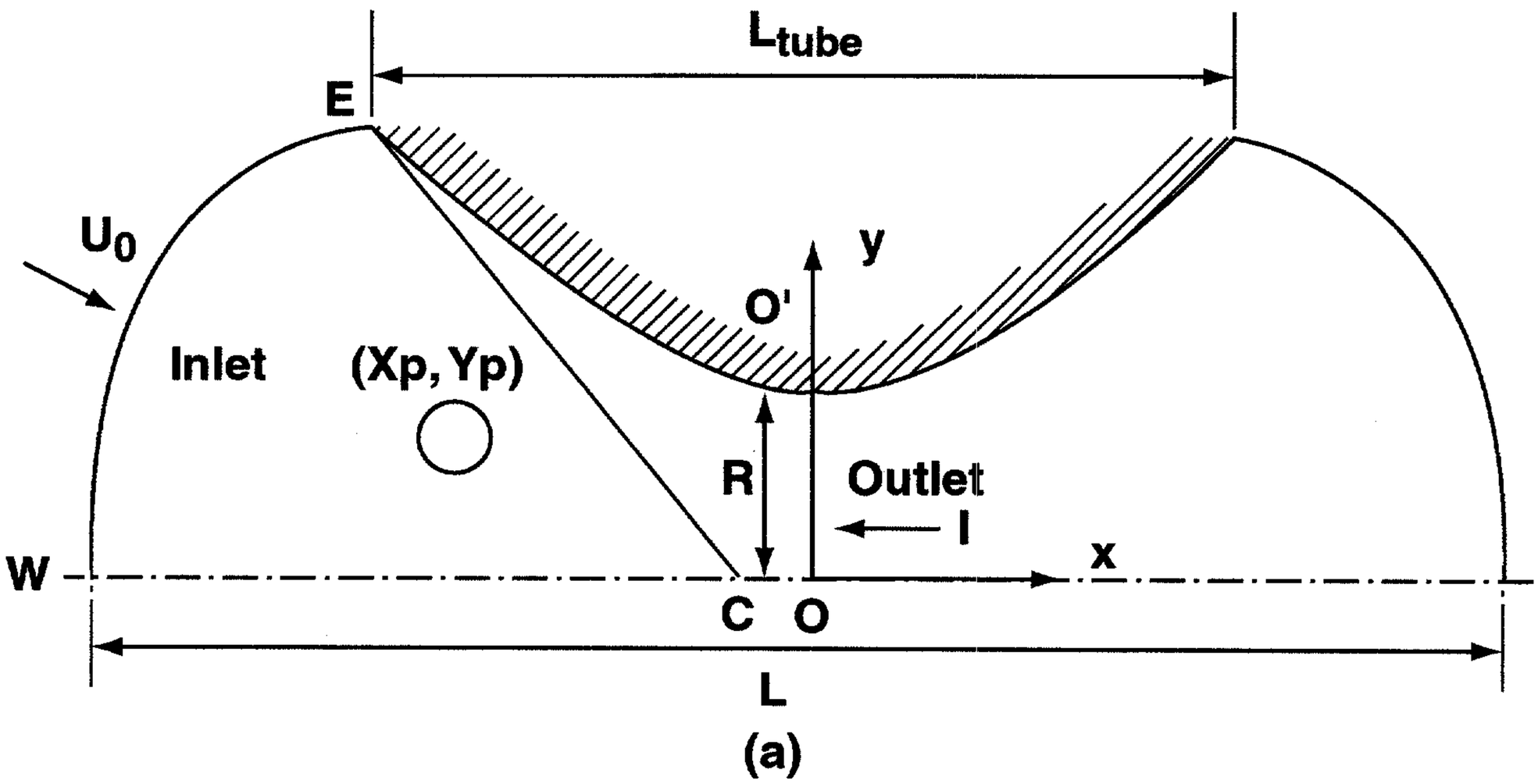
L_{tube}
E
U_0
Inlet
(Xp, Yp)
y
O'
R
Outlet
I
x
W
C
O
L
(a)

FIG. 4

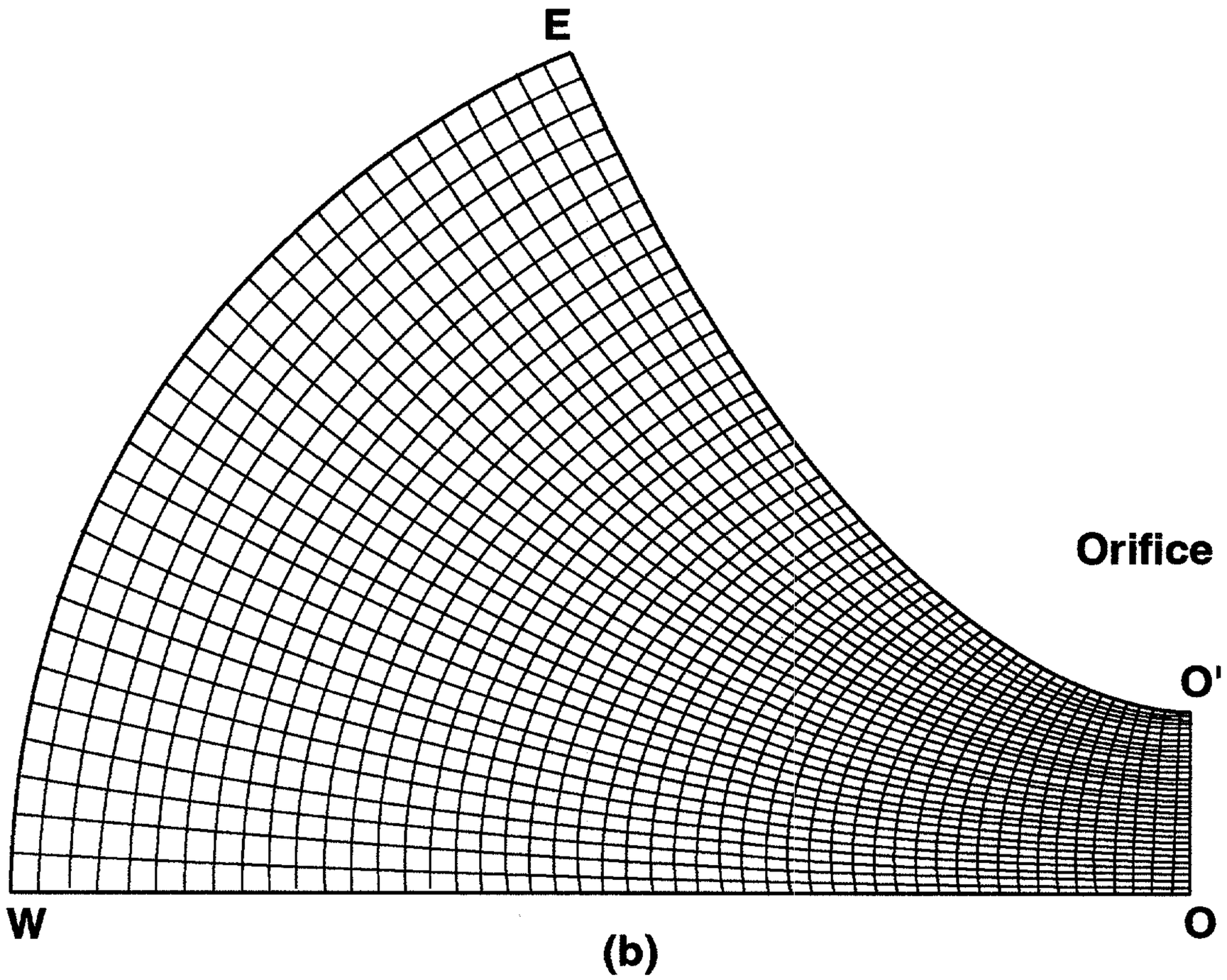
E
Orifice
O'
W
O
(b)

FIG. 5

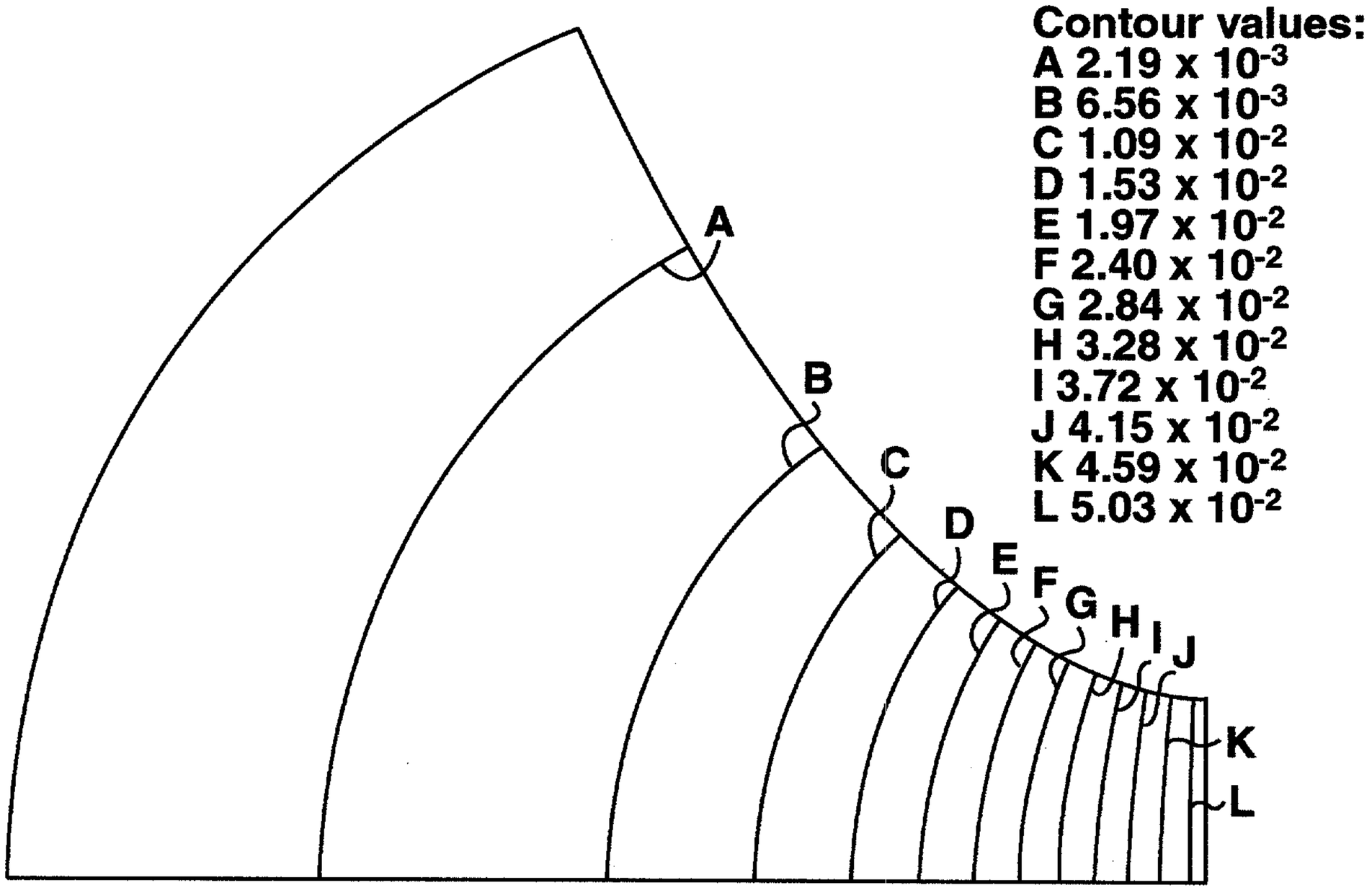
A
B
C
D
E
F
G
H
I
J
K
L
Contour values:
A 2.19 x 10-3
B 6.56 x 10-3
C 1.09 x 10-2
D 1.53 x 10-2
E 1.97 x 10-2
F 2.40 x 10-2
G 2.84 x 10-2
H 3.28 x 10-2
I 3.72 x 10-2
J 4.15 x 10-2
K 4.59 x 10-2
L 5.03 x 10-2
(a)

FIG. 6a

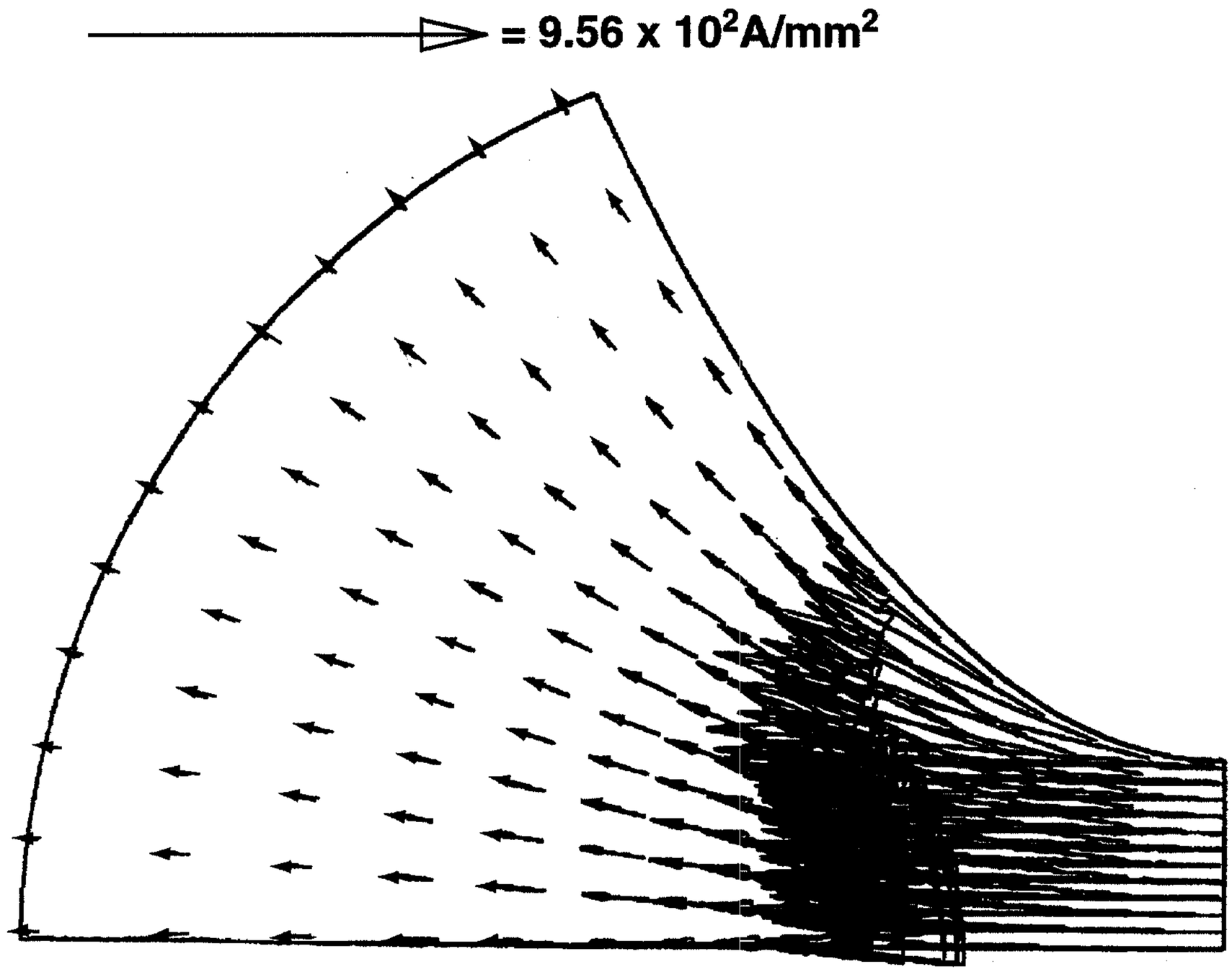

FIG. 6b

(b)

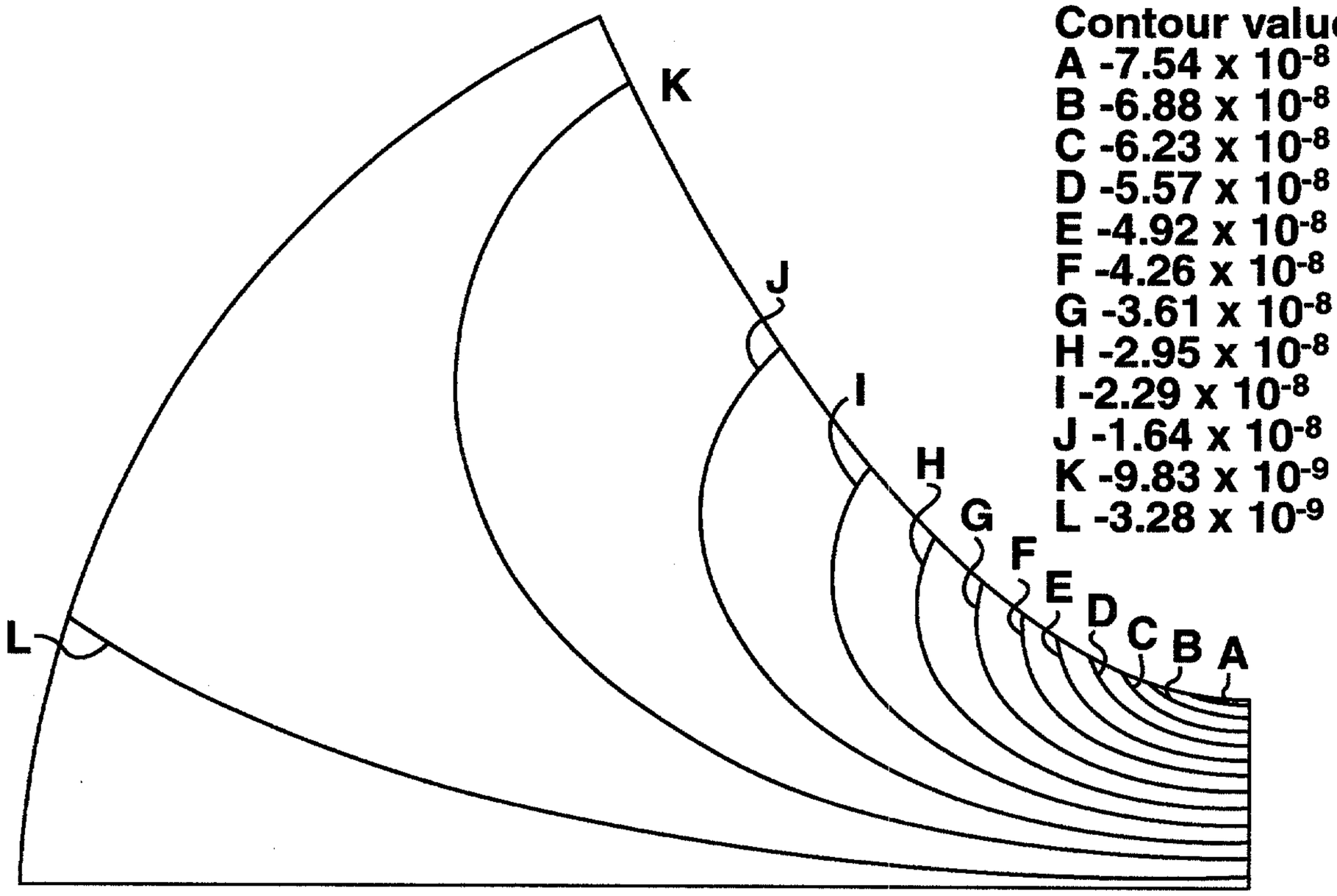

(c)

FIG. 6c

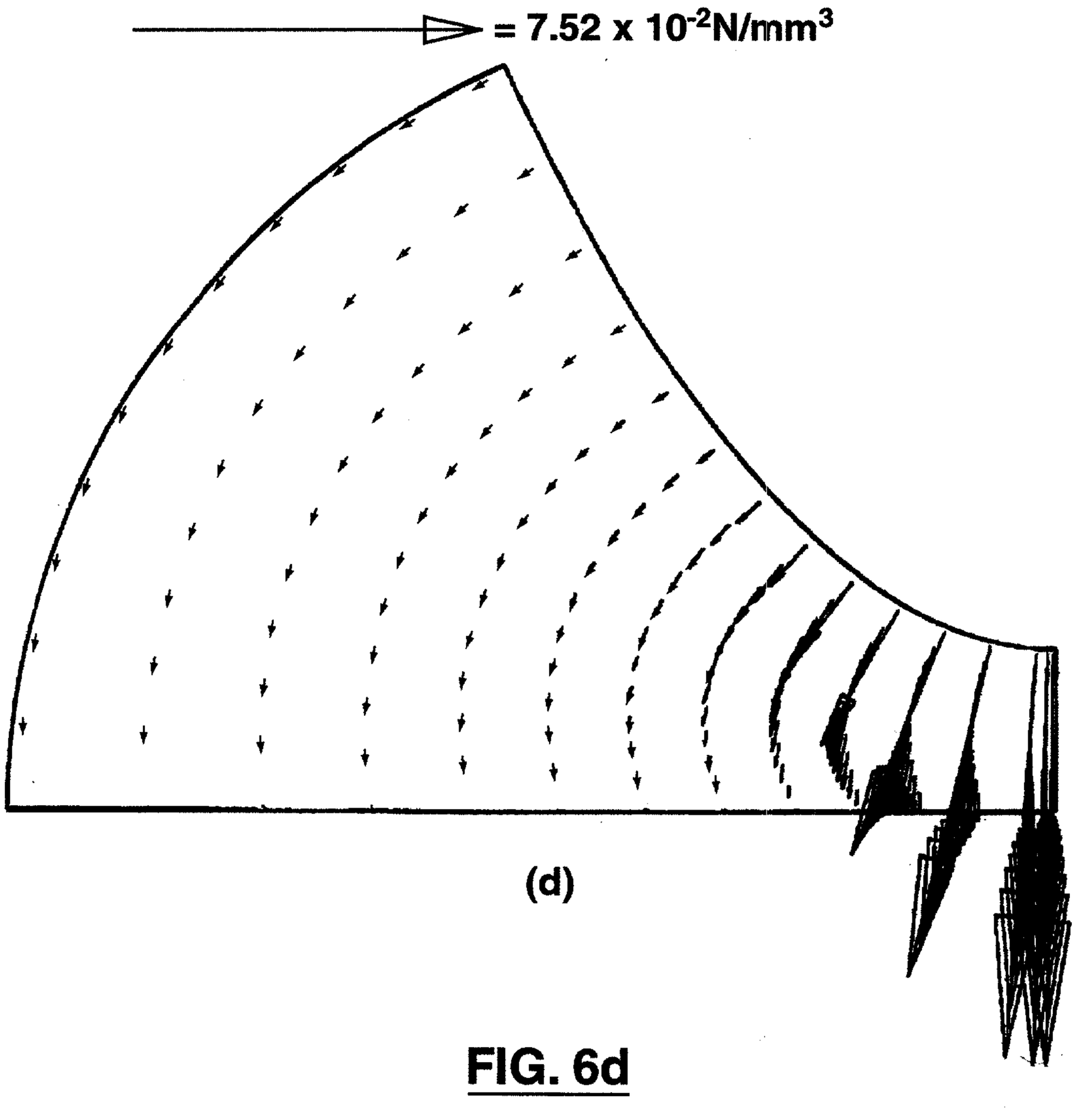

FIG. 6d

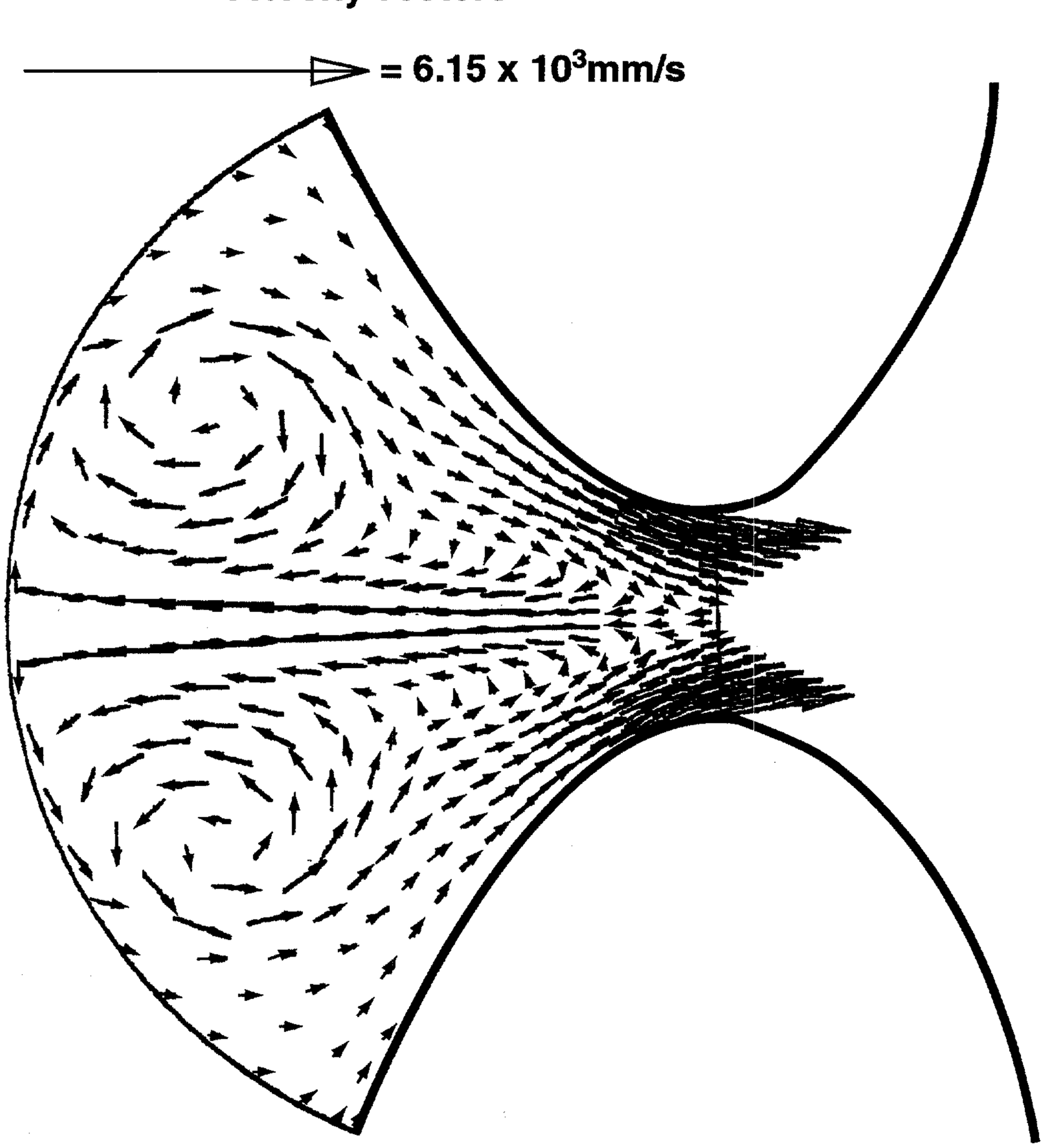

FIG. 7

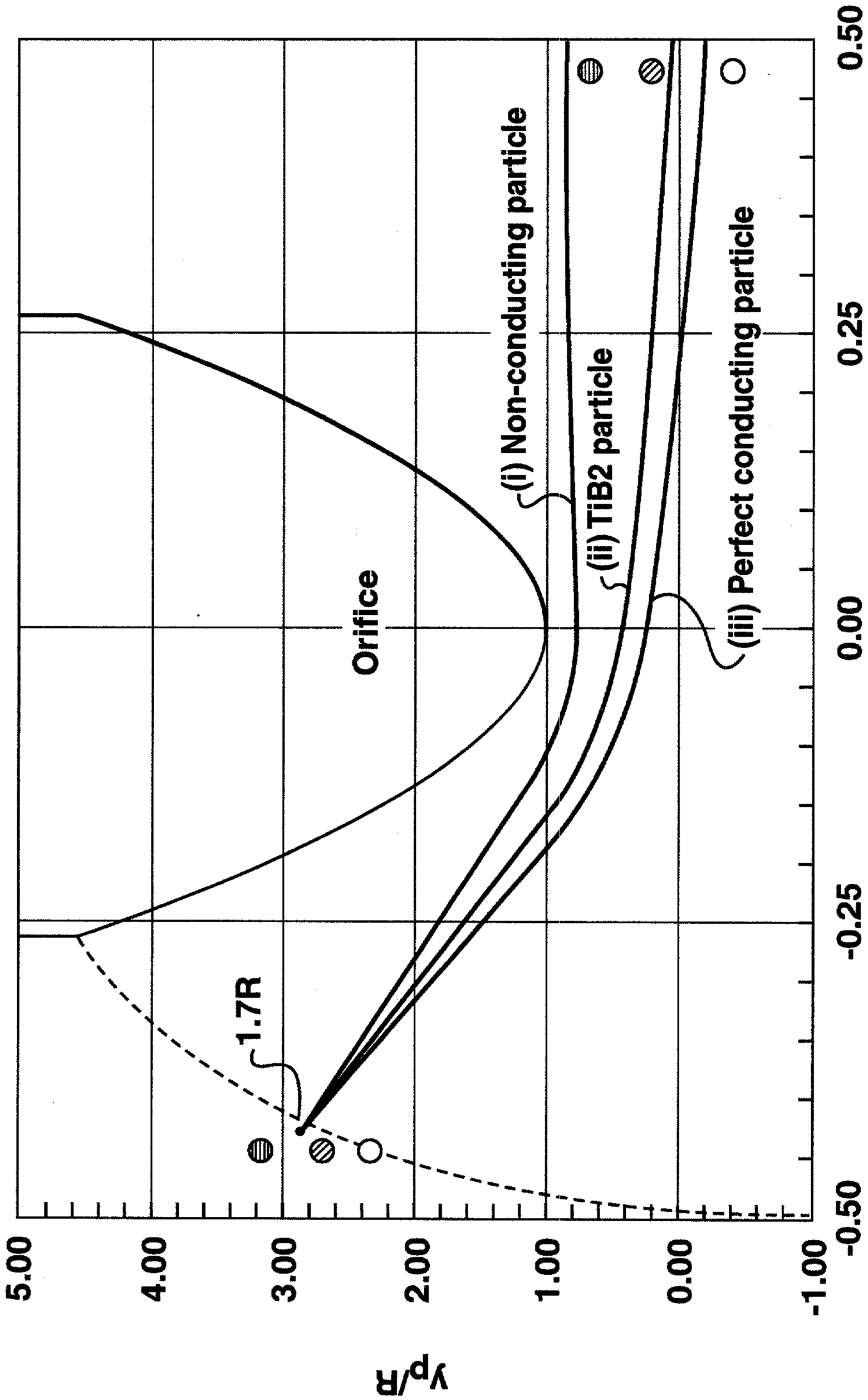
(i) Non-conducting particle
(ii) TiB2 particle
(iii) Perfect conducting particle
Orifice
1.7R
0.50
0.25
0.00
-0.25
-0.50
5.00
4.00
3.00
2.00
1.00
0.00
-1.00
x_p/L
y_p/R

FIG. 8

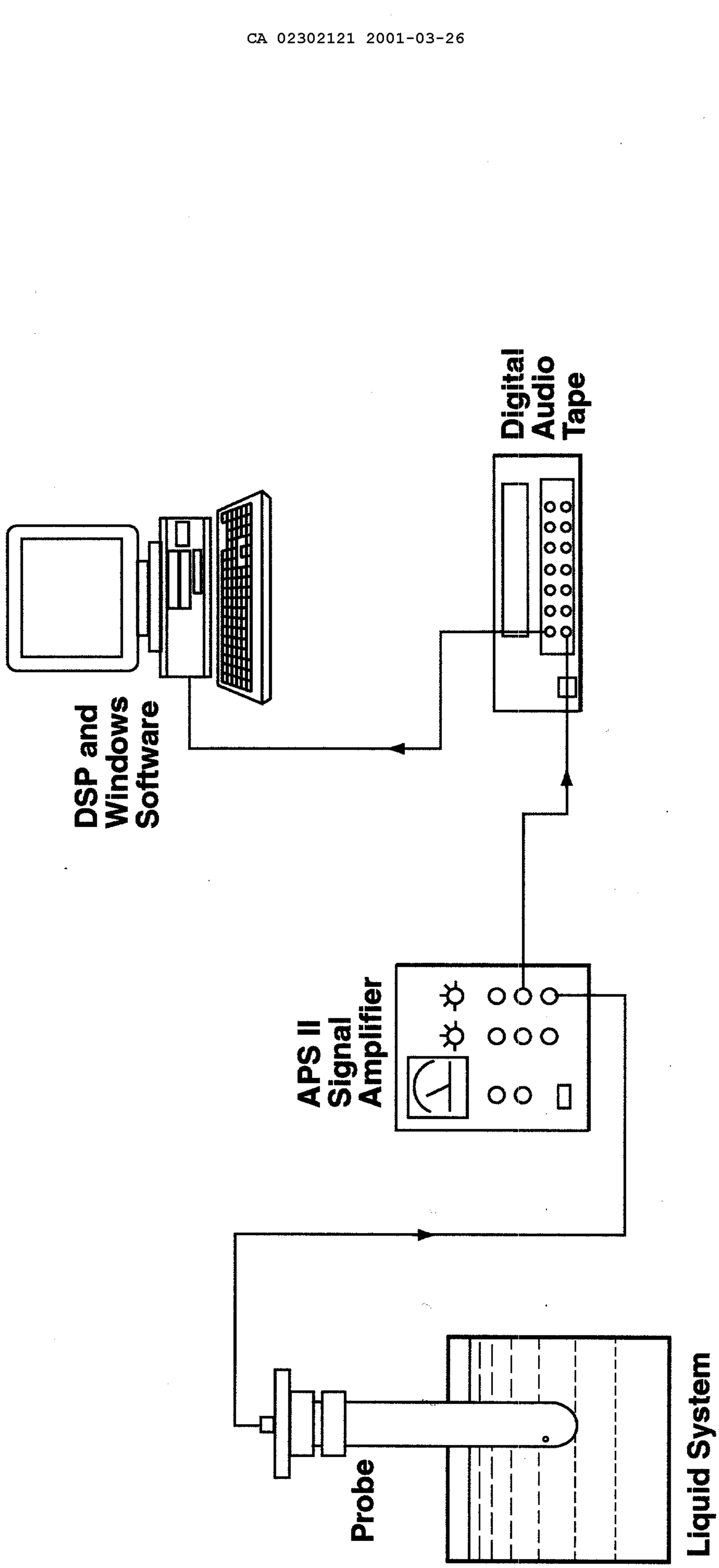
Digital
Audio
Tape
DSP and
Windows
Software
APS II
Signal
Amplifier
Probe
Liquid System

FIG. 9

Velocity Vectors

= 6.15 x 10^3mm/s